

Free-Free Gaunt factors for atmospheres of accreting pulsars observable with X-ray space missions

PARISEE S. SHIRKE ¹

¹*Inter-University Centre for Astronomy and Astrophysics
Post Bag 4, Ganeshkhind,
Pune 411 007, India*

ABSTRACT

Free-Free Gaunt factors for X-ray absorption by hot plasma in the presence of a strong magnetic field are reported. Modified formulae are used for application to the non-local thermodynamic equilibrium conditions found in accreting pulsar atmospheres. Given upcoming global X-ray polarimetric space missions, these can be used for the construction of an absorption matrix in discrete-ordinate polarised radiative transfer.

Keywords: (stars:) pulsars: general — X-rays: binaries — radiation mechanisms: thermal — plasmas — methods: numerical — stellar models

1. INTRODUCTION

The radiation scattering environment in a pulsar atmosphere is conventionally taken to be an accreted hot, tenuous, homogeneous plasma comprising mostly ionized hydrogen with trace helium (Meszaros & Nagel 1985a,b). Gaunt factors may need to be computed to account for photon-plasma interactions in the presence of a strong magnetic field using appropriate absorption and scattering cross-sections (Harding & Daugherty 1991) for determining the effective opacity and optical depth (See e.g. Meszaros et al. (1988) and references therein). The plasma consists of three different values of co-existent temperatures, namely (i) the plasma ion temperature, (ii) the electron temperature parallel to the magnetic field \vec{B} and (iii) the temperature representing the electron distribution over the Landau levels, which results in non-thermal local equilibrium (non-LTE) conditions. Continuous absorption is dominated by the free-free Bremsstrahlung process except near the cyclotron resonance (where resonant magneto-Compton scattering may set in).

Gaunt factors are slowly varying smooth functions that appear as multiplicative quantum mechanical corrections in the description of continuous (free-free or bound-free) absorption and emission (Rybicki & Lightman 1979) and were developed from the classical formula by Kramers (1923). These were introduced to provide a better description of stellar opacity arising from highly ionized plasma interactions in stellar interiors (Gaunt 1930) and were later named after their discoverer by Chandrasekhar (1939). Karzas & Latter (1961) have summarized the analytic formulae for computation of Gaunt factors at non-relativistic energies. Although recent works provide improved calculations of free-free Gaunt factors for astrophysical applications like radiative transfer in galaxy clusters, spectral distortions of CMB, and free-free galactic foreground (Chluba et al. 2020), this work computes the same in the context of accretion-powered pulsars.

2. METHODS

Gaunt factors appear in the expression for the magnetic free-free absorption coefficient (See Meszaros & Nagel (1985a,b); Ventura (1979)),

$$\alpha_i(\omega, \theta) = \alpha_0[\phi_+(\omega)|e_+^i|^2 g_\perp + \phi_-(\omega)|e_-^i|^2 g_\perp + \phi_z(\omega)|e_z^i|^2 g_\parallel] \quad (1)$$

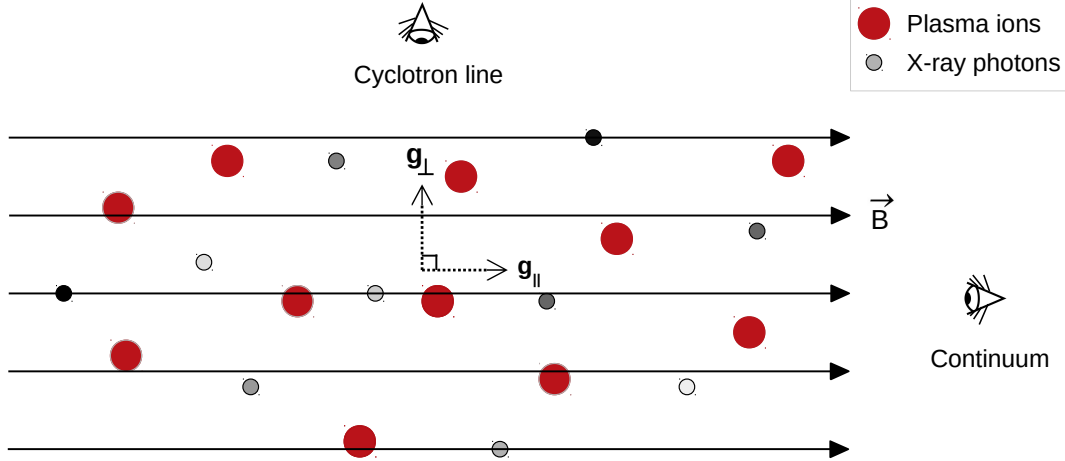


Figure 1. Sketch of a model pulsar atmosphere with a combination of accreted plasma ions and emitted thermal Bremsstrahlung X-ray photons. The direction of the dipolar magnetic field is perpendicular to the surface near the polar regions. Two gaunt factors (g_{\perp} and g_{\parallel}) are required to characterize the anisotropic X-ray photon absorption in the presence of a strong magnetic field. These correspond to the cyclotron line and X-ray continuum, respectively.

where α_0 is the non-magnetic free-free absorption coefficient measuring the free-free opacity of non-magnetized plasma given as,

$$\alpha_0 = \frac{4\pi^2 Z^2 \alpha^3 \hbar^2 c^2 N}{m_e \omega^3 \sqrt{\pi kT/2m_e}}, \quad (2)$$

and

$$\phi_{+,-,z} = \frac{3}{2} \frac{c}{r_0 \omega} |\text{Im } T_{+,-,z}|, \quad (3)$$

where Z represents the mean plasma atomic number, α is the fine structure constant ($= 1/137$), T is the plasma temperature ($= 8$ keV, 10 keV for plasma in model pulsar atmospheres) (Meszaros & Nagel 1985b), N is the number of electrons and ω is the incident spectral energy, $T_{+,-,z}$ are the components of the polarization tensor, r_0 is the electron classical radius along with standard physical constants.

To account for anisotropic effects due to the magnetic field, the Gaunt factors are resolved into two components as shown in Fig. 1: (i) for the cyclotron line g_{\perp} (See Nishimura (2008) for details on cyclotron line profiles) and (ii) the continuum g_{\parallel} . The direction of the magnetic field is the natural axis with respect to which the directions in the suffixes are defined. The modified expressions to incorporate a non-LTE situation (Nagel 1980) are,

$$g_{\perp}(\omega, \omega_c, T_{\parallel}) = \int_{-\infty}^{\infty} C_1 \left(\frac{\omega}{\omega_c} e^{2x} \right) e^{-\frac{\hbar\omega}{kT_{\parallel}} \sinh^2 x} dx \quad (4)$$

$$g_{\parallel}(\omega, \omega_c, T_{\parallel}) = 2 \int_{-\infty}^{\infty} \left(\frac{\omega}{\omega_c} e^{2x} \right) C_0 \left(\frac{\omega}{\omega_c} e^{2x} \right) e^{-\frac{\hbar\omega}{kT_{\parallel}} \sinh^2 x} dx \quad (5)$$

where C_1 and C_0 are Coulomb matrix elements defined by Virtamo & Jauho (1975), representing the strength of transition from the n^{th} to n^{th} Landau level. These values are tabulated in Ventura (1973) as W_{00} and W_{10} for parameter values ranging from $z = 0.01 - 10.00$, with z being defined as,

$$z = \frac{1}{4\gamma} [\beta^2 + (\Delta K)^2] \quad (6)$$

where, $\gamma = \frac{1}{2} eB/\hbar c$, $\beta^2/4\gamma$ is the screening parameter and $\Delta K = k' - k$ represents the momentum transfer.

For a known value of model plasma temperature T_{\parallel} , the Gaunt factors are functions of the X-ray spectral energy ω and the systemic cyclotron energy ω_c , where the latter is fixed for a particular system but can vary from pulsar

to pulsar. Using $kT = 8$ keV for model accreting pulsar atmospheres (See Appendix), the integrals are computed¹ using $z = \frac{\omega}{\omega_c} e^{2x}$ and reading off the corresponding value of W_{00} and W_{10} for each x , using linear interpolation, if required. The sufficiency of the range of Ventura’s z values was separately confirmed by verifying that the integrands have vanishingly small values outside this range (by evaluating the Gaunt integrals with Coulomb matrix elements set to fixed constants).

The cyclotron energies ω_c in Tables 1 and 2 are initially have discrete sampling across the full range of pulsar magnetic field strengths ($B = 10^{11} - 10^{13}$ Gauss). The resultant set of values subsumes the model cyclotron energies of 38 keV and 50 keV used by Meszaros & Nagel (1985a) and Meszaros & Nagel (1985b). On the other hand, the range of spectral energies ω in Tables 1, 2 is initially kept consistent with the discrete set of values used in Meszaros & Nagel (1985a)’s radiative transfer computations. Both are later allowed to continuously span the full observing band of broad-band X-ray space missions, $\omega = 1 - 100$ keV and pulsar magnetic field strengths $\omega_c = 1 - 120$ keV at a fine spectral resolution of $\Delta\omega = 0.1$ keV. Recursive adaptive Simpson’s quadrature is used to perform the integration since it provides results – with error bars – consistent with those obtained using other integrators² while using a number of iterations, N close to the default value recommended for the integration module. The preliminary criteria for the choice of N is that a change to $2N$ should not produce a change in the results of Gaunt factor values within 1% accuracy.

3. RESULTS AND DISCUSSIONS

Tables 1 and 2 and Fig. 2 show the computation results for the values of Gaunt factors, g_{\perp} for pulsar cyclotron lines and g_{\parallel} for X-ray continua. Since cyclotron resonance scattering features tend to be sharp, the energy band was sampled with a fine resolution ($\Delta\omega = 0.1$ keV) for close sampling, especially near the cyclotron line energy (ω_c). As seen in Fig. 2, the Gaunt factors exhibit their typical smooth behaviour. There are no discontinuities, even near the cyclotron resonant energies which otherwise produce sharp scattering features in X-ray pulsar spectra. Both the Gaunt factors are seen to decrease with the X-ray photon energy as mentioned in Ventura et al. (1979). g_{\perp} increases with an increase in magnetic field strength whereas g_{\parallel} is seen to exhibit the reverse trend, getting suppressed with an increase in the magnetic field strength. It would be a trivial exercise to represent these results – plotted as per convention in Fig. 2 for maintaining consistency with existing reports in the literature – as Gaunt functions on a 3-D grid with spectral energy ω and the cyclotron energy ω_c as the choice of X and Y axes.

Table 1. Modified anisotropic Gaunt factor, g_{\perp} for a model Meszaros & Nagel plasma temperature of 8 keV (*columns*) over the full range of source pulsar magnetic field strengths, $B = 10^{11} - 10^{13}$ G with discrete sampling for ω_c including model Meszaros & Nagel values and (*rows*) model Meszaros & Nagel energies for ω .

Energy ' ω '	Cyclotron energy ' ω_c ' (keV)						
(keV)	1.0	20.0	38.0	50.0	77.0	96.0	116.0
1.58	5.300323	41.53	44.68945	45.2593	45.31703	44.96964	44.471494
3.85	0.640098	20.74975	31.43405	35.39241	40.17336	41.83082	42.813269
8.98	0.066791	4.15618	8.714412	11.805245	18.307305	22.234345	25.737028
18.37	0.006339	0.910697	2.097411	2.940173	4.896875	6.305912	7.811599
29.13	0.000714	0.33181	0.797979	1.151917	2.015293	2.649239	3.326339
38.59	0.000087	0.180185	0.440854	0.639782	1.143135	1.528293	1.948742
51.71	0.000002	0.093834	0.240337	0.349771	0.627453	0.845317	1.09022
84.66	0.0	0.028196	0.084971	0.128962	0.233738	0.314034	0.405335

¹ Using dimensional analysis, \hbar is hereby omitted from the exponent in the implementation. Both the numerator, ω and denominator, kT are in units of keV. The cyclotron energy, ω_c in the following expression for z is also in keV.

² <https://scipy.org> (Virtanen et al. 2020). See Sec. *Software*.

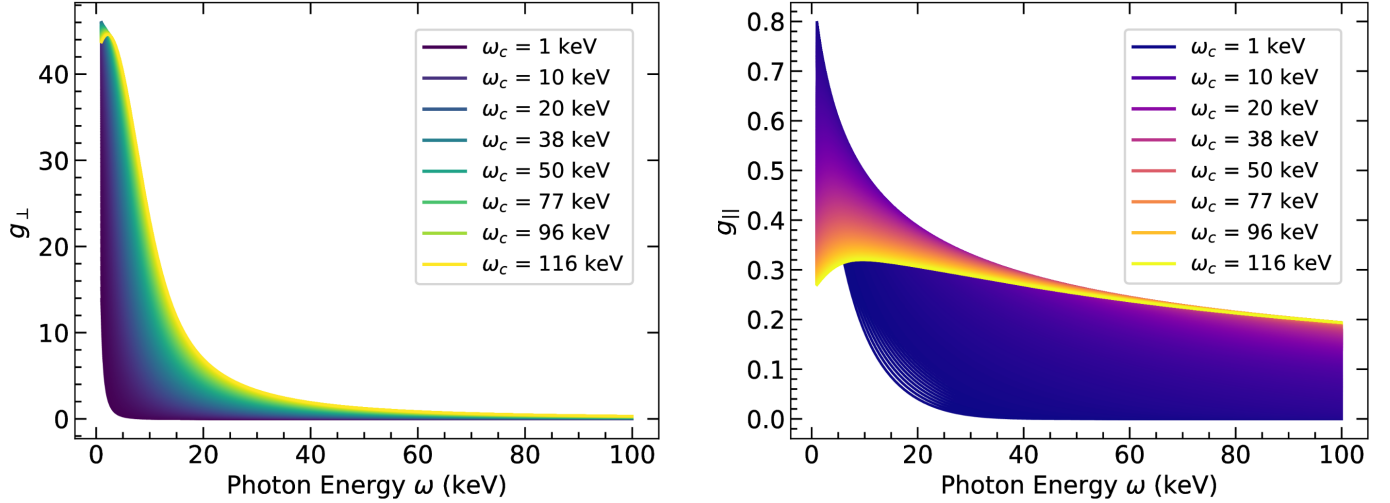


Figure 2. Modified anisotropic Gaunt functions (*left*) g_{\perp} and (*right*) g_{\parallel} for the full spectral range of broad-band X-ray space missions i.e. the full observing range of X-ray photons energies, $\omega = 1 - 100$ keV and (*isochors*) the full span of source pulsar magnetic field strengths, $B = 10^{11} - 10^{13}$ G sampled at a fine spectral resolution of $\Delta\omega = \Delta\omega_c = 0.1$ keV for a plasma temperature of $kT = 8$ keV.

Table 2. Modified anisotropic Gaunt factor, g_{\parallel} for a model Meszaros & Nagel plasma temperature of 8 keV (*columns*) over the full range of source pulsar magnetic field strengths, $B = 10^{11} - 10^{13}$ G with discrete sampling for ω_c including model Meszaros & Nagel values and (*rows*) model Meszaros & Nagel energies for ω .

Energy ' ω ' (keV)	Cyclotron energy ' ω_c ' (keV)						
	1.0	20.0	38.0	50.0	77.0	96.0	116.0
1.58	0.693441	0.580327	0.470625	0.422493	0.3486	0.31256	0.282872
3.85	0.457043	0.570444	0.483836	0.441327	0.371953	0.33657	0.306753
8.98	0.202961	0.50167	0.45561	0.427458	0.376749	0.34888	0.324334
18.37	0.051592	0.398091	0.3917	0.37875	0.348874	0.330137	0.312663
29.13	0.008675	0.317857	0.33395	0.330488	0.315196	0.303548	0.291772
38.59	0.001224	0.266875	0.295343	0.296937	0.289336	0.281716	0.273456
51.71	0.000038	0.213812	0.25377	0.260534	0.259949	0.25582	0.250702
84.66	0.0	0.134059	0.180778	0.196641	0.208867	0.209444	0.208118

4. CONCLUSIONS

Bremsstrahlung Gaunt factors – used in the studies of electrodynamics and radiative processes – are presented over the complete broad-band X-ray observing range of $\omega = 1 - 100$ keV for the full span of accreting pulsar magnetic field strengths, $B = 10^{11} - 10^{13}$ Gauss ($\omega_c = 1 - 120$ keV) with (i) discrete sampling for model values and (ii) continuous sampling at a fine spectral resolution of 0.1 keV for a model plasma temperature of 8 keV. The results are shown in Fig. 2.

Since accreting X-ray pulsars are promising non-terrestrial physics laboratories, this, in general, characterizes the physics of magnetically confined (X-ray pulsar) plasmas, particularly, their interactions with incident high energy radiation in vacuum. Exploiting the naturally-occurring condition of a high-velocity accreted plasma funneled by a strong dipolar pulsar magnetic field and interacting with thermal Bremsstrahlung X-ray radiation, the free-free Gaunt factors for a hot ($T_{\parallel} = 8$ keV), magnetized ($B = 10^{11} - 10^{13}$ G) plasma in non-LTE conditions, including anisotropic effects (g_{\perp} , g_{\parallel}) are presented for 1 – 100 keV X-ray photon (ω) absorption in model pulsar atmospheres. A new, custom numerical tool ‘Gaunt Factor Calculator’ is developed for the same.

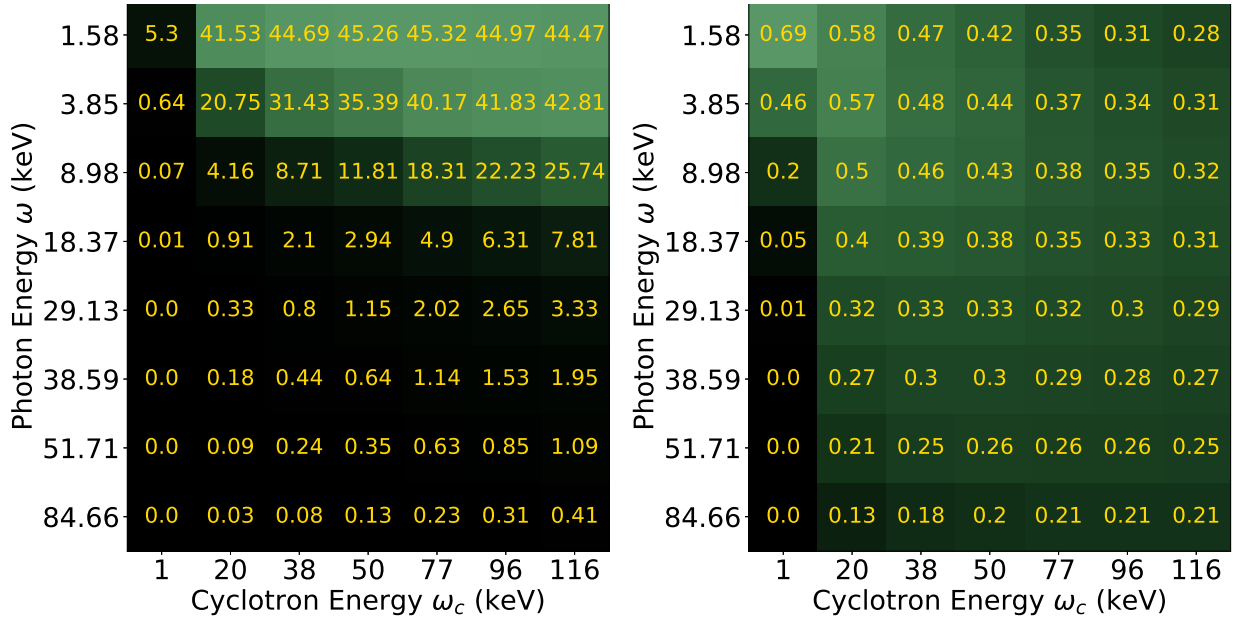


Figure 3. Modified anisotropic Gaunt maps (*left*) g_{\perp} and (*right*) g_{\parallel} for source pulsar magnetic field strengths, $B = 10^{11} - 10^{13}$ G with discrete sampling for ω_c and model X-ray photon energies ω consistent with Meszaros & Nagel (1985b) for a plasma temperature $kT = 8$ keV. In each grid, relatively larger values are represented by brighter shades.

The author would like to thank Prof. D. Bhattacharya and Prof. D. Mukherjee for useful discussions, suggestions and ideas and Prof. G. C. Dewangan for support.

Facilities: Dell OptiPlex 5060 Desktop³ with an Intel[®] Core[™] i7-8700T processor, Ubuntu[®] 18.04.3 LTS (64-bit) Operating System, 8 GB DDR4 RAM & 2 TB HDD.

Software: NumPy⁴ Ver 1.16.4 (Harris et al. 2020), SciPy⁵ Ver 1.3.0 (Virtanen et al. 2020), Matplotlib⁶ Ver 3.1.0 (Hunter 2007) packages in Jupyter environment (Kluyver et al. 2016) for Python 3 (Van Rossum & Drake 2009), the SAO/NASA Astrophysics Data System⁷, e-Print arXiv⁸.

APPENDIX

A. VISUAL REPRESENTATION

Fig. 3 depicts the values computed in Tables 1 and 2 as color maps for a visual representation of the trend in the figures.

B. VARIATION WITH PLASMA TEMPERATURE

The variation of the Gaunt factors can also be studied with a change in the third parameter of plasma temperature, kT_{\parallel} (Rybicki & Lightman 1979). Apart from the model value of $kT_{\parallel} = 8$ keV used by Meszaros & Nagel – results for which are displayed in Sec. 3 – Yahel (1979a) suggest electron temperatures of 4 – 50 keV for hot strongly magnetized plasma in pulsar atmospheres with an emphasis on the 10 – 20 keV range. In an earlier work, Yahel (1979b) discarded temperatures above 10 keV for Her X-1. Fig. 4 shows the change in the anisotropic Gaunt curves with plasma temperatures sampled within Yahel’s range.

³ https://www.dell.com/learn/in/en/inbsd1/shared-content~data-sheets~en/documents~optiplex_5060_spec_sheet.pdf

⁴ <https://numpy.org>

⁵ <https://scipy.org>

⁶ <https://matplotlib.org>

⁷ <https://ui.adsabs.harvard.edu/>

⁸ <https://arxiv.org/>

The computed results exhibit a variation with the plasma temperature. On comparative inspection, it is observed that the steep fall in the Gaunt curves tends to flatter slopes for hotter plasma. The g_{\parallel} curves in Fig. 4 exhibit an increasing upward offset whereas the $g_{\perp}(\omega_c = 1 \text{ keV})$ curve rises to a higher value near the lower X-ray photon energy end ($\omega = 1 \text{ keV}$).

REFERENCES

- Chandrasekhar, S. 1939, *An introduction to the study of stellar structure* (Dover Publications)
- Chluba, J., Ravenni, A., & Bolliet, B. 2020, *MNRAS*, 492, 177, doi: [10.1093/mnras/stz3389](https://doi.org/10.1093/mnras/stz3389)
- Gaunt, J. A. 1930, *Philosophical Transactions of the Royal Society of London. Series A, Containing Papers of a Mathematical or Physical Character*, 229, 163
- Harding, A. K., & Daugherty, J. K. 1991, *ApJ*, 374, 687, doi: [10.1086/170153](https://doi.org/10.1086/170153)
- Harris, C. R., Millman, K. J., van der Walt, S. J., et al. 2020, *Nature*, 585, 357, doi: [10.1038/s41586-020-2649-2](https://doi.org/10.1038/s41586-020-2649-2)
- Hunter, J. D. 2007, *Computing in Science & Engineering*, 9, 90, doi: [10.1109/MCSE.2007.55](https://doi.org/10.1109/MCSE.2007.55)
- Karzas, W. J., & Latter, R. 1961, *ApJS*, 6, 167, doi: [10.1086/190063](https://doi.org/10.1086/190063)
- Kluyver, T., Ragan-Kelley, B., Pérez, F., et al. 2016, in *Positioning and Power in Academic Publishing: Players, Agents and Agendas*, ed. F. Loizides & B. Schmidt (IOS Press), 87–90. <https://eprints.soton.ac.uk/403913/>
- Kramers, H. A. 1923, *The London, Edinburgh, and Dublin Philosophical Magazine and Journal of Science*, 46, 836
- Meszaros, P., & Nagel, W. 1985a, *ApJ*, 298, 147, doi: [10.1086/163594](https://doi.org/10.1086/163594)
- . 1985b, *ApJ*, 299, 138, doi: [10.1086/163687](https://doi.org/10.1086/163687)
- Meszaros, P., Novick, R., Szentgyorgyi, A., Chanan, G. A., & Weisskopf, M. C. 1988, *ApJ*, 324, 1056, doi: [10.1086/165962](https://doi.org/10.1086/165962)
- Nagel, W. 1980, *ApJ*, 236, 904, doi: [10.1086/157817](https://doi.org/10.1086/157817)
- Nishimura, O. 2008, *ApJ*, 672, 1127, doi: [10.1086/523782](https://doi.org/10.1086/523782)
- Rybicki, G. B., & Lightman, A. P. 1979, *Radiative processes in astrophysics* (Wiley-Interscience Publication, New York)
- Van Rossum, G., & Drake, F. L. 2009, *Python 3 Reference Manual* (Scotts Valley, CA: CreateSpace)
- Ventura, J. 1973, *Phys. Rev. A*, 8, 3021, doi: [10.1103/PhysRevA.8.3021](https://doi.org/10.1103/PhysRevA.8.3021)
- Ventura, J. 1979, *PhRvD*, 19, 1684, doi: [10.1103/PhysRevD.19.1684](https://doi.org/10.1103/PhysRevD.19.1684)
- Ventura, J., Nagel, W., & Meszaros, P. 1979, *ApJL*, 233, L125, doi: [10.1086/183090](https://doi.org/10.1086/183090)
- Virtamo, J., & Jauho, P. 1975, *Nuovo Cimento B Serie*, 26, 537, doi: [10.1007/BF02738576](https://doi.org/10.1007/BF02738576)
- Virtanen, P., Gommers, R., Oliphant, T. E., et al. 2020, *Nature Methods*, 17, 261. <http://dx.doi.org/10.1038/s41592-019-0686-2>
- Yahel, R. Z. 1979a, *A&A*, 78, 136
- . 1979b, *ApJL*, 229, L73, doi: [10.1086/182933](https://doi.org/10.1086/182933)

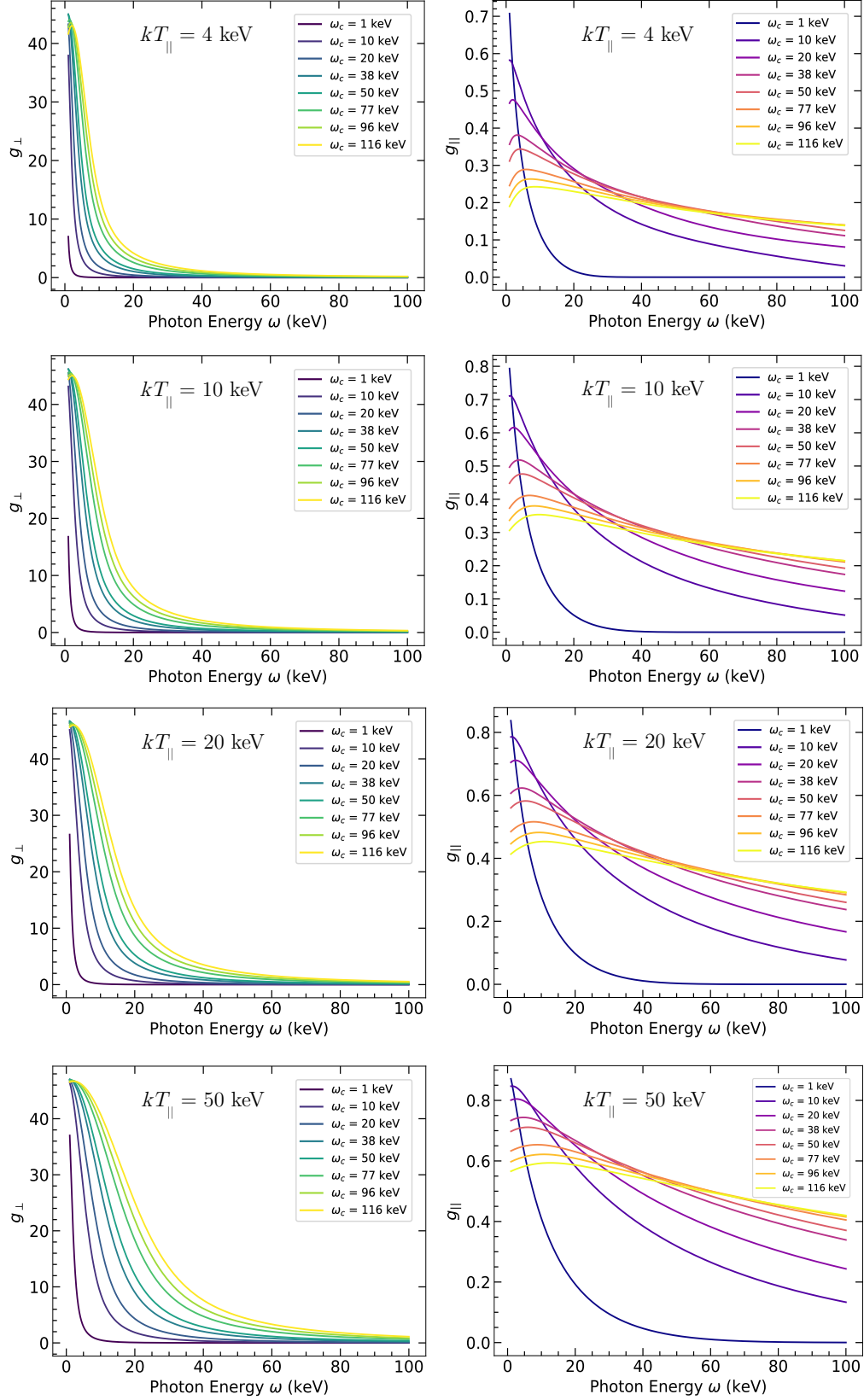


Figure 4. Modified Gaunt curves (*left column*) $g_{\perp}(\omega)$ and (*right column*) $g_{\parallel}(\omega)$ for the full spectral range of X-ray space missions *i.e.* photon energies, $\omega = 1 - 100$ keV with $\Delta\omega = 0.1$ keV with (*isochors*) discrete sampling over the full range of source magnetic field strengths, $B = 10^{11} - 10^{13}$ G including model Meszaros & Nagel values for (*top to bottom*) increasing model plasma temperatures of $kT_{\parallel} = 4, 10, 20$ and 50 keV in Yahel's range.